

Lattice thermal conductivity of self-assembled PbTe-Sb₂Te₃ composites with nanometer lamellae

Teruyuki Ikeda¹, Eric S. Toberer¹, Vilupaur A. Ravi², Sossina M. Haile¹, G. Jeffrey Snyder¹

¹California Institute of Technology

1200 E. California Blvd., Pasadena, CA 91106, USA

²California State Polytechnic University

3801 W. Temple Avenue, Pomona, CA 91768, USA

Abstract

In the system of PbTe and Sb₂Te₃, a metastable compound Pb₂Sb₆Te₁₁ appears by solidification processing. It has been reported that this compound is decomposed into the two immiscible thermoelectric materials forming nanosized lamellar structure by heat treatments. The fraction transformed and the inter-lamellar spacing was systematically investigated. In this work, the thermal conductivities and the electrical resistivities have been measured as functions of annealing time through the transformation and the coarsening processes to clarify the effect of the fraction transformed and the inter-lamellar spacing. The thermal conductivity of Pb₂Sb₆Te₁₁ is lower than that after the decomposition. The lattice part of the thermal conductivity of PbTe/Sb₂Te₃ lamellar samples decreases with decreasing inter-lamellar spacing. This is considered to be due to the coarsening of the microstructure.

Introduction

In order for thermoelectric devices to be more commonly used in large industrial fields for effective use of heat or electrical energy, it is essential to discover materials with a high thermoelectric figure of merit, zT , defined as $S^2\sigma T/\kappa$, where S is the Seebeck coefficient, σ the electrical conductivity and κ the thermal conductivity. One way to improve a figure of merit zT is to introduce nano-sized structure into thermoelectric materials [Cay05, Ven01, Har03]. This is achieved presumably by enhanced phonon scattering [Che04], which decreases thermal conductivity κ . Here, we examine a system of two immiscible thermoelectric materials: PbTe-Sb₂Te₃. In this system, it has been shown that the metastable compound Pb₂Sb₆Te₁₁ appears at a composition close to that of the eutectic [Abr65, Ike06] and decomposes into two thermoelectric compounds, PbTe and Sb₂Te₃, forming nano-sized lamellar structures [Ike07a, Ike07b]. In the present work, eutectic PbTe-Sb₂Te₃ alloys were synthesized by quenching in a copper mold and then annealed at several temperatures to control the fraction transformed and inter-lamellar spacing. The electrical resistivity and the thermal conductivity of as-quenched and annealed samples have been investigated as functions of the spacing.

Experimental procedure

Samples with overall composition matching the Pb₂Sb₆Te₁₁ compound (Pb_{10.5}Sb_{31.6}Te_{57.9}) were prepared by injection molding. Stoichiometric quantities of Pb, Sb, and Te granules were loaded into 12mm fused silica ampoules and then sealed under a vacuum of approximately 4×10^{-3} Pa to prevent oxidation at high temperatures. Samples were then melted in vertical furnace for 5 min and were subsequently

water quenched. They were then cut into small pieces with diamond saw. The small pieces of 15-20 g in total were put into a fused silica tube with 12 mm outer diameter and with a hole of approximately 1 mm diameter and were melted by induction heating under vacuum of approximately 4×10^{-3} Pa. When the sample melted, the sample dropped through the hole into a copper mold of $20 \times 30 \times \text{mm}^3$. For property measurements, samples with size of typically $10 \times 10 \text{ mm}^2$ were cut out with diamond saw and then the surfaces were ground to remove the surface layers until the final thickness was around 1.5 mm.

Electrical resistivity and thermal conductivity measurements were carried out before and after annealing the samples. For annealing, samples were sealed under vacuum in fused silica tubes. Annealing temperature was 673 K (78 h, 150 h) or 773 K (1 h, 24 h, 126 h).

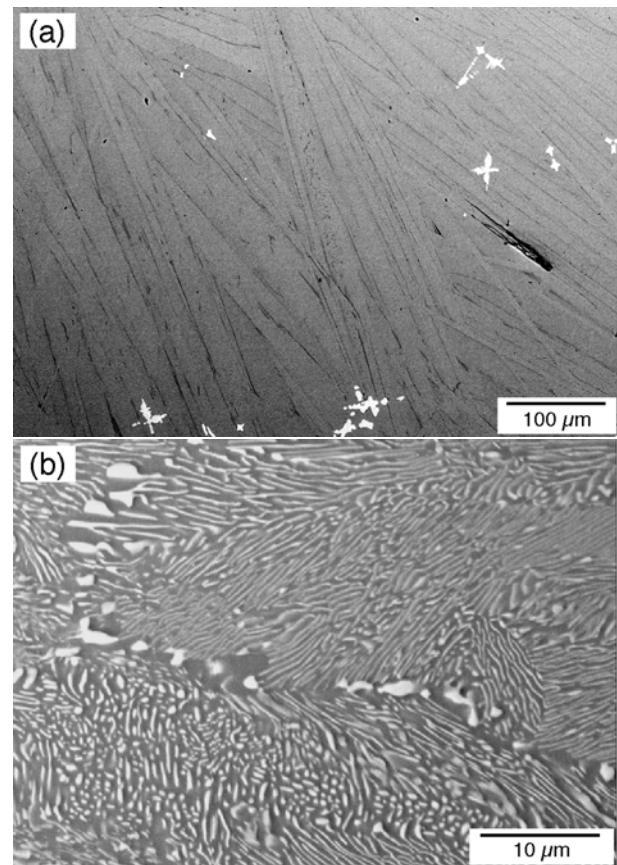


Figure 1: Microstructure of Pb_{10.5}Sb_{31.6}Te_{57.9}: (a) as quenched and (b) annealed at 673 K for 150 h.

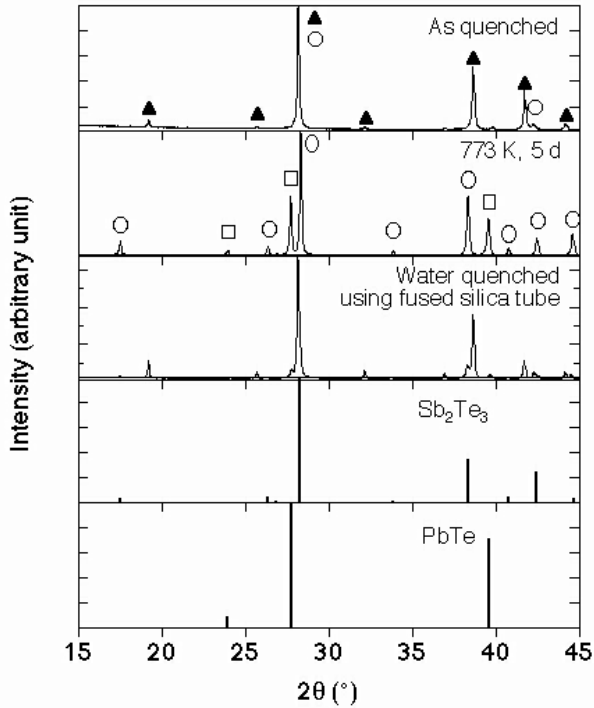


Figure 2: XRD profiles obtained from $\text{Pb}_{10.5}\text{Sb}_{31.6}\text{Te}_{57.9}$ as quenched and annealed at 773 K for 5 days. Open squares (\square), open circles (\circ) and solid triangles (\blacktriangle) show the peaks from PbTe, Sb_2Te_3 and $\text{Pb}_2\text{Sb}_6\text{Te}_{11}$ phases, respectively.

The electrical resistivity (ρ) was measured up to 523 K, below which microstructure is not considered to practically change during measurements because of low atomic diffusivity [Ike07b], using the van der Pauw method with a current of 10 mA as functions of temperature.

The thermal diffusivities were measured up to 523 K using the same samples as the electrical resistivity measurements by flash diffusivity technique (LFA457, NETSZCH). The thermal conductivity (κ) was calculated from the thermal diffusivity which was experimentally measured and the heat capacity which was estimated using Dulong-Petit law.

The microstructures were observed using field emission-scanning electron microscope (Carl Zeiss LEO 1550 VP) equipped with a backscattered electron (BSE) detector for its high compositional contrast capabilities. The accelerating voltage was 20 kV. The microstructures were digitally analyzed using an image analysis program (Macscope, Mitani Corp.) to determine the inter-lamellar spacing (ILS) and the fraction transformed (Y). X-ray diffraction (XRD) experiments (Phillips X-Pert Pro diffractometer, Cu K- α radiation, $15^\circ \leq 2\theta \leq 45^\circ$) were performed directly on the as-prepared ingots to identify phases.

Results and discussion

Microstructure

Figure 1 (a) and (b) show the microstructure of the samples which are as-quenched and after annealing at 673 K for 150 h, respectively. The sample in as-quenched state is almost composed of the gray matrix phase, $\text{Pb}_2\text{Sb}_6\text{Te}_{11}$. The thin dark acicular phase is Sb_2Te_3 and the bright dendrites are

PbTe. The phases composing of as-quenched and annealed samples were also confirmed by XRD experiments as shown in Fig. 2. These features were consistent with the solidification microstructure of this system by water-quenching using fused silica tubes [Ike06]. The inter-lamellar spacing in the solidification structure was 13 μm in the vicinity of the sample surface and 16 μm in the middle, which were also consistent with that for water quenching using fused silica tube in the previous work. After annealing at 673 K for 78 h or at 773 K 126 h, $\text{Pb}_2\text{Sb}_6\text{Te}_{11}$ is almost completely decomposed to Sb_2Te_3 and PbTe as reported in the previous work [Ike07a]. The backscattered electron images were digitally analyzed to determine the fraction transformed (Y) and the inter-lamellar spacing (ILS). The results of the image analysis is summarized in Table 1. In the sample annealed at 673 K for 78 or 150 h and the one annealed at 773 K for 126 h, the transformation to PbTe/ Sb_2Te_3 lamellar structure is almost complete. It is also found that ILS is increased by annealing.

Table 1. Fraction transformed (Y) and inter-lamellar spacing (ILS) of the samples annealed at 673 or 773 K.

Sample ID	Annealing condition		Y (%)	ILS (nm)	
	T / K	t / h		Average	Standard deviation
A	673	78	99.7	536	155
		150	100	575	153
B	773	1	88.7	544	168
		126	100	1591	487

Electrical resistivity

Figure 3 shows the electrical resistivity and the carrier concentration measured as functions of temperature. The resistivity is found to decrease by the decomposition of $\text{Pb}_2\text{Sb}_6\text{Te}_{11}$ to PbTe/ Sb_2Te_3 lamellae. This is mainly due to the increase in carrier concentration. It is also found that the electrical resistivity is not significantly affected in the coarsening process.

Thermal conductivity

Figure 4 shows the temperature dependence of thermal conductivity of sample B, which was annealed at 773 K for 1 h, 24 h and 126 h. The thermal conductivities (κ_{tot}) were calculated from the measured thermal diffusivity (α), the measured density (ρ), and the heat capacity (C_p) evaluated by Dulong-Petit law using the relation, $\kappa_{\text{tot}} = \rho C_p \alpha$. The electron part of the thermal conductivity, κ_{el} was evaluated by Wiedemann-Franz law, $\kappa_{\text{el}} = LT/\rho$, where L is Lorenz number. Moreover, the lattice part of the thermal conductivity, κ_{lat} , was calculated using $\kappa_{\text{tot}} = \kappa_{\text{el}} + \kappa_{\text{lat}}$. The lattice part of the thermal conductivity in the as-quenched state, *i.e.* that of $\text{Pb}_2\text{Sb}_6\text{Te}_{11}$, is significantly lower than those after the decomposition. While the electrical resistivity is almost

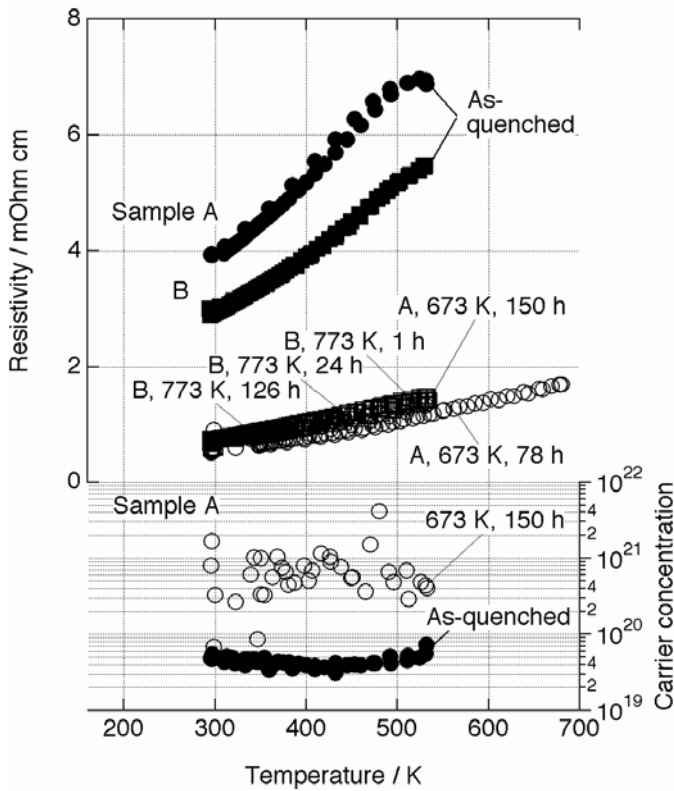


Figure 3: Electrical resistivity and carrier concentration of $\text{Pb}_{10.5}\text{Sb}_{31.6}\text{Te}_{57.9}$ in the as-quenched state and after annealings at 673 K or 773 K.

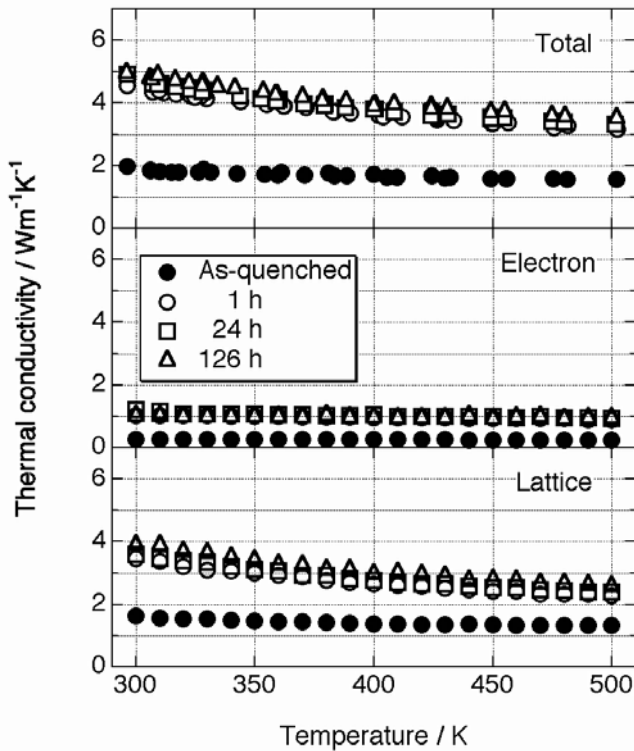


Figure 4: Total, electronic part, and lattice part of the thermal conductivity of $\text{Pb}_{10.5}\text{Sb}_{31.6}\text{Te}_{57.9}$ in the as-quenched state and after annealing at 773 K.

constant after annealing for 1 h at 773 K, the thermal conductivity slightly increases. As seen in the figure, this is due to the increase of lattice part of the thermal conductivity. As shown in Table 1, the microstructure is coarsened by annealing. That is qualitatively consistent with the previous work [Ike07b]. Thus, the increase in the lattice part of the thermal conductivity could be attributed to the lowering of phonon scattering at phase boundaries due to the coarsening of microstructure. The significantly low thermal conductivity of $\text{Pb}_2\text{Sb}_6\text{Te}_{11}$ could be considered to be due to the strong effect of phonon scattering.

Figure 5 shows the ILS dependence of the lattice thermal conductivity of $\text{Pb}_2\text{Sb}_6\text{Te}_{11}$ and $\text{PbTe}/\text{Sb}_2\text{Te}_3$ lamellar composites. In the figure, the spacing of $\text{Pb}_2\text{Sb}_6\text{Te}_{11}$ was taken to be 1.4 nm, which is the period of similar atomic stacking in the crystal structure [She04]. Lattice part of the thermal conductivity is lowered with decrease in ILS and the reduction the lattice thermal conductivity ultimately reaches that of $\text{Pb}_2\text{Sb}_6\text{Te}_{11}$, which has a periodical layered crystal structure. Therefore, it is again considered that the reduction of the lattice thermal conductivity with the decrease of ILS is due to the enhancement of phonon scattering at phase boundaries. Thus, it is concluded that there is a significant effect of the nanosized lamellar structure on the reduction of lattice thermal conductivity.

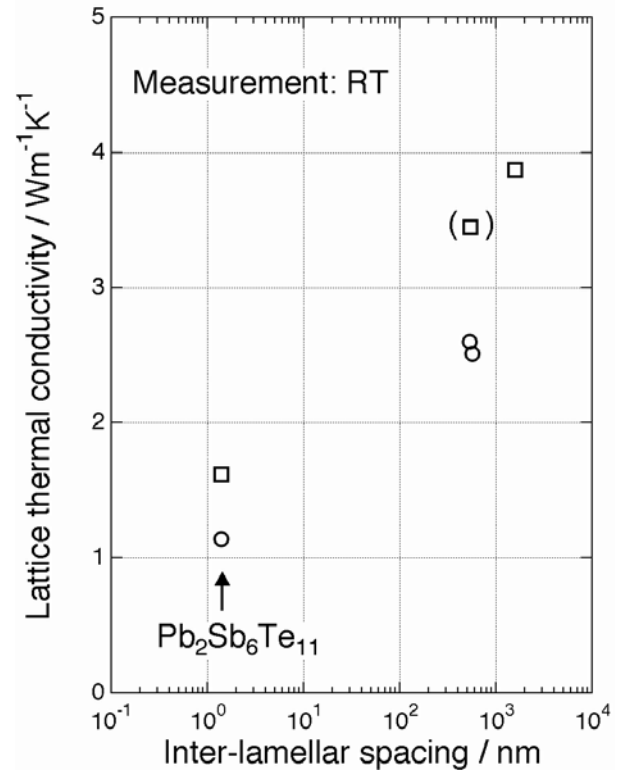


Figure 5: The dependence of lattice thermal conductivity of $\text{PbTe}/\text{Sb}_2\text{Te}_3$ lamellar composites and $\text{Pb}_2\text{Sb}_6\text{Te}_{11}$ on inter-lamellar spacing. Circles and Squares show the results from samples sample A and B, respectively. The spacing for $\text{Pb}_2\text{Sb}_6\text{Te}_{11}$ was taken to be the period of similar atomic stacking (1.4 nm) in the crystal structure [She04].

Conclusions

$\text{Pb}_{10.5}\text{Sb}_{31.6}\text{Te}_{57.9}$ (the composition corresponding to $\text{Pb}_2\text{Sb}_6\text{Te}_{11}$) samples were prepared by solidification processing using copper mold. After the solidification, the sample was mainly composed of $\text{Pb}_2\text{Sb}_6\text{Te}_{11}$. $\text{Pb}_2\text{Sb}_6\text{Te}_{11}$ was decomposed to PbTe and Sb_2Te_3 by annealing at 673 or 773 K. The fraction transformed and the inter-lamellar spacing (540-1600 nm) were controlled by annealing period. The electrical resistivity and the thermal conductivity were measured before and after annealing. It was found that the electrical resistivity is the highest for $\text{Pb}_2\text{Sb}_6\text{Te}_{11}$ (without annealing). Then, the electrical resistivity decreases as the decomposition to $\text{PbTe}/\text{Sb}_2\text{Te}_3$ lamellae proceeds. The thermal conductivity increases as the decomposition proceeds and the resulting nanostructure is coarsened.

Acknowledgments

This work was supported by the Office of Naval Research and Jet Propulsion Laboratory.

References

- Abr65 Abrikosov, N. K. *et al.*, "The System $\text{PbTe-Sb}_2\text{Te}_3$," *Inorg. Mater.* Vol. 1 (1965), pp. 1944-1946.
- Ike06 Ikeda, T. *et al.*, "Solidification Processing of Alloys in the Pseudo-binary $\text{PbTe-Sb}_2\text{Te}_3$ System," *Acta Mater.* Vol. 55 (2007), pp. 1227-1239.
- Ike07a Ikeda, T. *et al.*, "Self-Assembled Nanometer Lamellae of Thermoelectric PbTe and Sb_2Te_3 with Epitaxy-like Interfaces," *Chem. Mater.* Vol. 19 (2007), pp. 763-767.
- Ike07b Ikeda, T. *et al.*, "Development and Evolution of Nanostructure in Bulk Thermoelectric Pb-Te-Sb Alloys," *J. Electr. Mater.*, in press.
- Cay05 Caylor, J. C. *et al.*, "Enhanced Thermoelectric Performance in PbTe -based Superlattice Structures from Reduction of Lattice Thermal Conductivity," *Appl. Phys. Lett.* Vol. 87 (2005), p. 023105.
- Ven01 Venkatasubramanian, R. *et al.*, "Thin Film Thermoelectric Devices with High Room-Temperature Figures of Merit," *Nature* 413 (2001), pp. 597-602.
- Har03 Harman, T. C. *et al.*, "Quantum Dot Superlattice Thermoelectric Materials and Devices," *Science* Vol. 297 (2003), pp. 2229-2232.
- Che04 Chen, G., Proc Ninth Intersociety Conference on Thermal and Thermomechanical Phenomena In Electronic Systems 2004 (IEEE Cat. No.04CH37543); p.8.
- She04 Shelimova, L. E. *et al.*, "Synthesis and structure of layered compounds in the $\text{PbTe-Bi}_2\text{Te}_3$ and $\text{PbTe-Sb}_2\text{Te}_3$ systems," *Inorg Mater.* Vol. 40 (2004), pp. 1264-1270.